บทความวิจัย

ผลของเลขสวอร์ลต่อเสถียรภาพของเปลวไฟในหัวเผาแก๊ส LPG แบบหมุนวนภายใต้สภาวะเปลวไฟอิสระ

สุเมธา ศรีบุญ อนิรุตต์ มัทธุจักร์* ชาคริต โพธิ์งาม และ ธนรัฐ ศรีวีระกุล
ภาควิชาวิศวกรรมเครื่องกล คณะวิศวกรรมศาสตร์ มหาวิทยาลัยอุบลราชธานี
ชยุต นันทดุสิต
ภาควิชาวิศวกรรมเครื่องกล คณะวิศวกรรมศาสตร์ มหาวิทยาลัยสงขลานครินทร์
สุทธิศักดิ์ พงศ์ธนาพาณิช
ภาควิชาเทคโนโลยีวิศวกรรมเครื่องกล วิทยาลัยเทคโนโลยีอุตสาหกรรม มหาวิทยาลัยเทคโนโลยีพระจอมเกล้าพระนครเหนือ

* ผู้นิพนธ์ประสานงาน โทรศัพท์ 0 4535 3309 อีเมล: Anirut.m@ubu.ac.th DOI: 10.14416/j.kmutnb.2026.09.003
รับเมื่อ 17 กันยายน 2568 แก้ไขเมื่อ 24 มกราคม 2569 ตอบรับเมื่อ 3 เมษายน 2569 เผยแพร่ออนไลน์ 7 กันยายน 2569
© 2026 King Mongkut's University of Technology North Bangkok. All Rights Reserved.

บทคัดย่อ

หัวเผาชนิดหมุนวนถูกนำมาใช้อย่างแพร่หลายในงานด้านพลังงานและอุตสาหกรรม เนื่องจากสามารถช่วยเพิ่มการผสมเชื้อเพลิงและอากาศได้ดี และสร้างความเสถียรให้กับเปลวไฟ อย่างไรก็ตามความเข้าใจอย่างลึกซึ้งเกี่ยวกับการเผาไหม้ของก๊าซปิโตรเลียมเหลว (LPG) ในหัวเผาแบบผสมก่อนชนิดหมุนวนภายใต้สภาวะเปลวไฟอิสระยังมีอยู่อย่างจำกัด ดังนั้นงานวิจัยนี้จึงมีวัตถุประสงค์ในการศึกษาพฤติกรรมการเผาไหม้ของเตาเผาแบบผสมล่วงหน้าที่ใช้เชื้อเพลิง LPG โดยถึงอิทธิผลของอัตราส่วนสมมูล (ϕ) ค่าเรย์โนลด์ (Re) และค่า swirl number ต่อโครงสร้างเปลวไฟ และเสถียรภาพการเผาไหม้ด้วยวิธีพลศาสตร์ของไหลเชิงคำนวณ (CFD) จากการใช้สมการการอนุรักษ์มวล โมเมนตัม พลังงาน และการขนส่งสปีชีส์ ร่วมกับแบบจำลองการเผาไหม้แบบผสมล่วงหน้าบางส่วน และแบบจำลองความปั่นป่วน RNG $k-\varepsilon$ รวมถึงแบบจำลองการถ่ายเทรังสี Discrete Ordinates โดยผลการจำลองได้ถูกตรวจสอบความถูกต้องกับผลทดลองพบว่ามีค่าเฉลี่ยความคลาดเคลื่อน 8.19% ซึ่งแสดงทำให้แบบจำลองมีความน่าเชื่อถือ โดยการจำลองจะศึกษาอิทธิพลของ Re = 2,000 4,000 และ 6,000 และอัตราส่วนสมมูล = 0.8 1.0 และ 1.2 จากผลการวิเคราะห์พบว่าการเผาไหม้บาง (ϕ = 0.8) เปลวไฟแบบมีลักษณะเรียวยาว โดยที่เปลวไฟจากการเผาไหม้ที่สโตอิชิโอเมตริก (ϕ = 1.0) มีลักษณะเปลวกะทัดรัด และสมมาตร ส่วนเปลวไฟแบบการเผาไหม้หนา (ϕ = 1.2) มีโซนปฏิกิริยาที่หนาแน่นขึ้น โดยการเพิ่มค่า Re ส่งผลให้การผสมเชื้อเพลิง อากาศ และความเสถียรของเปลวไฟดีขึ้น โดยเงื่อนไข Re = 6,000 และ ϕ = 0.8 ให้ค่า swirl number สูงสุด และก่อให้เกิดบริเวณหมุนวนตรงกลางที่แข็งแรงทำให้เปลวไฟยึดเกาะได้มั่นคง และมีอุณหภูมิสูงสุดเท่ากับ 2,079 เคลวิน ผลการศึกษานี้ได้ยืนยันว่าค่า swirl number เป็นพารามิเตอร์สำคัญในการออกแบบหัวเผาแบบผสมล่วงหน้าเพื่อเพิ่มประสิทธิภาพการเผาไหม้และเสถียรภาพของเปลวไฟ อีกทั้งยังสามารถใช้เป็นแนวทางในการพัฒนาหัวเผาเชื้อเพลิง LPG ในระดับอุตสาหกรรมได้อย่างมีประสิทธิภาพ

คำสำคัญ: โครงสร้างเปลวไฟ พลศาสตร์ของไหลเชิงคำนวณ หัวเผาแบบผสมก่อนชนิดหมุนวน Swirl number

การอ้างอิงบทความ: สุเมธา ศรีบุญ, อนิรุตต์ มัทธุจักร์, ชาคริต โพธิ์งาม, ธนรัฐ ศรีวีระกุล, ชยุต นันทดุสิต และ สุทธิศักดิ์ พงศ์ธนาพาณิช, "ผลของเลขสวอร์ลต่อเสถียรภาพของเปลวไฟในหัวเผาแก๊ส LPG แบบหมุนวนภายใต้สภาวะเปลวไฟอิสระ," *วารสารวิชาการพระจอมเกล้าพระนครเหนือ*, ปีที่ 36, ฉบับที่ 4, หน้า 1–16, ต.ค.–ธ.ค. 2569. เลขที่บทความ 264-058313, doi: 10.14416/j.kmutnb.2026.09.003.

Research Article

Influence of Swirl Number on Flame Stability of an LPG Premixed Swirl Burner under Free-Flame Conditions

Sumeta Sribun, Anirut Matthujak*, Chakrit Pongarm and Thanarath Sriveerakul
Department of Mechanical Engineering, Faculty of Engineering, Ubon Ratchathani University, Ubon Ratchathani, Thailand
Chayut Nuntadusit
Department of Mechanical Engineering, Faculty of Engineering, Prince of Songkla University, Songkhla, Thailand
Sutthisak Phongthanapanich
Department of Mechanical Engineering Technology, College of Industrial Technology, King Mongkut's University of Technology North Bangkok, Bangkok, Thailand

* Corresponding Author, Tel. 0 4535 3309, E-mail: Anirut.m@ubu.ac.th DOI: 10.14416/j.kmutnb.2026.09.003
Received 17 September 2025; Revised 24 January 2026; Accepted 3 April 2026; Published online: 7 September 2026
© 2026 King Mongkut's University of Technology North Bangkok. All Rights Reserved.

Abstract

Swirl burners are widely used in energy and industrial applications due to their ability to enhance fuel–air mixing and stabilize flames. However, a detailed understanding of Liquefied Petroleum Gas (LPG) combustion in premixed swirl burners under free-flame conditions remains limited. Free-flame operation minimizes wall-confinement effects and allows clearer observation of intrinsic swirl-induced flame stabilization mechanisms. This study numerically investigates the combustion behavior of an LPG-fueled premixed swirl burner, focusing on the effects of equivalence ratio, Reynolds number, and swirl number on flame structure and stability. Computational Fluid Dynamics (CFD) simulations were performed by solving the governing equations of mass, momentum, energy, and species transport. Turbulence was modeled using the RNG k–ε approach, while combustion was represented by the partially premixed combustion model coupled with the discrete ordinates radiation model. The numerical model was validated against experimental data, showing good agreement with a mean error of 8.19%, indicating its reliability. Simulations were conducted for Reynolds numbers of 2,000, 4,000 and 6,000 and equivalence ratios of 0.8, 1.0 and 1.2. The results indicate that lean flames are elongated, stoichiometric flames are compact and symmetric, and rich flames exhibit thicker reaction zones. Increasing Reynolds number improves fuel–air mixing and flame stability. The condition at Reynolds number 6,000 and equivalence ratio 0.8 yields the highest swirl number, producing a strong central recirculation zone, a well-anchored flame, and a maximum temperature of 2,079 K. These findings confirm that swirl number is a key parameter in the design of premixed swirl burners to improve combustion efficiency and flame stability.

Keywords: Flame Structure, Computational Fluid Dynamics, Premixed Swirl Burner, Swirl Number

Please cite this article as: S. Sribun, A. Matthujak, C. Pongarm, T. Sriveerakul, C. Nuntadusit, and S. Phongthanapanich, "Influence of swirl number on flame stability of an LPG premixed swirl burner under free-flame conditions," *The Journal of KMUTNB*, vol. 36, no. 4, pp. 1–16, Oct.–Dec. 2026 (in Thai), Art. no. 264-058313, doi: 10.14416/j.kmutnb.2026.09.003

1. Introduction

Combustion in swirling flows is widely used in burner and combustor design because swirl enhances fuel–air mixing and promotes stable flame anchoring through the formation of a Central Recirculation Zone (CRZ) [1]–[4]. Accordingly, swirl burners are commonly applied in industrial furnaces, gas turbines, and laboratory-scale combustors. A clear understanding of swirl-stabilized flame structures is therefore essential for developing combustion systems that are both efficient and operationally safe. Liquefied Petroleum Gas (LPG), mainly composed of propane and butane, is widely used in domestic and industrial sectors due to its favorable combustion characteristics and broad availability. Several experimental studies have investigated premixed LPG flames, focusing on flame structure, temperature distribution, and heat-transfer performance under different operating conditions [5], [6]. Although these experiments provide valuable insight, they often offer limited spatial resolution and may not fully capture complex turbulence-combustion interactions.

As a result, Computational Fluid Dynamics (CFD) is frequently employed as a complementary approach to obtain detailed information on flow and combustion fields that can be difficult or impractical to measure experimentally [7]–[9]. Nevertheless, CFD predictions require validation against experimental data to ensure reliability and accuracy [10], [11]. Recent studies have demonstrated the capability of CFD for analyzing swirl-stabilized flames, premixed combustion processes, and associated thermal–flow characteristics [1], [9], [12]–[15].

In premixed swirl combustion, the Reynolds number (Re) is a key nondimensional parameter governing turbulence intensity and fuel–air mixing, and thus strongly influencing flame structure and stabilization. At low Reynolds numbers, weaker turbulence limits mixing and reduces flame anchoring. As Reynolds number increases, enhanced turbulent fluctuations and shear-layer development strengthen the swirl-induced recirculation zone and promote the transport of hot products toward the flame root, improving flame anchoring and resistance to lift-off or blow-off.

Despite these advances, LPG-fueled swirl flames under free flame conditions remain relatively underexplored. Importantly, most prior swirl-combustion studies have focused on confined flames (where wall effects influence recirculation and stabilization) or on other fuel types, leaving free-flame LPG premixed swirl combustion less directly examined. Many previous investigations emphasize confined flames or alternative fuels, which can obscure intrinsic stabilization behavior due to wall-confinement effects. Free flame configurations reduce these confinement influences and allow the fundamental stabilization mechanisms such as swirl-induced recirculation and turbulence–chemistry interaction to be examined more directly.

In this study, CFD simulations are used to investigate the combustion characteristics of an LPG-fueled premixed swirl burner under free flame operation. The numerical model is validated against experimental temperature data reported by Uppatam *et al.* [5] to confirm prediction reliability. The analysis considers a burner height of 23 mm and examines Reynolds numbers of 2,000, 4,000 and 6,000 together with equivalence ratios of 0.8, 1.0 and 1.2. By systematically evaluating flame structure and stability across these conditions, this work provides new insight into LPG premixed swirl combustion in free-flame operation and offers practical guidance for designing efficient and stable industrial burners.

2. Materials and Methods

2.1 Experimental Reference

The numerical model was validated using the experimental dataset of Uppatam *et al.* [5], selected because it closely corresponds to the present study in burner type, fuel composition, and operating regime. Their experiments examined premixed LPG/air swirl flames under free-flame (free-jet) conditions using LPG composed of 70% propane and 30% butane, with Reynolds numbers of 2,000, 4,000 and 6,000 and equivalence ratios of 0.8, 1.0 and 1.2. The burner geometry (20 mm outlet diameter, 5 mm throat diameter, and 23 mm chamber height; H/D = 4.6) is consistent with the configuration adopted in the present simulations. All geometric and operating parameters used for validation are summarized in Table 1. The use of free-flame operation minimizes wall-confinement effects, making this reference particularly suitable for assessing CFD accuracy and capturing intrinsic swirl-stabilized flame behavior.

2.2 Model and Parameters

The swirl burner employed in this study is a commercially available market product, rather than a newly designed or customized component. The burner geometry and operating characteristics were adopted directly from the manufacturer’s specifications and the experimental reference used for validation. Accordingly, the numerical model was constructed to accurately represent the actual configuration of this commercial burner, ensuring that the simulation results are directly applicable to practical burner operation and

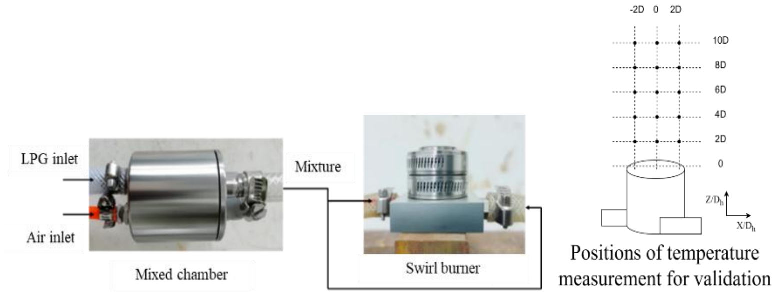

Figure 1 Mixing chamber and swirl burner used in the study.

industrial combustion systems.

Figure 1 shows the premixed swirl burner system used in this study, comprising a cylindrical mixing chamber and a swirl burner with two opposing tangential inlets to generate strong swirl. The mixing chamber (50 mm diameter and 50 mm length) ensures premixing of LPG (70% propane and 30% butane by volume) with air before entering the burner, which has a 20 mm outlet diameter and a chamber height of 23 mm. The corresponding geometric parameters are listed in Table 1.

Based on the experimental reference in section 2.1, simulations were performed at Reynolds numbers of 2,000, 4,000 and 6,000 and equivalence ratios of 0.8, 1.0 and 1.2 (Table 1) to represent lean, stoichiometric, and rich premixed conditions across different turbulence levels. Reynolds number primarily controls turbulence intensity and mixing, which influences shear-layer development and flame anchoring via swirl-induced recirculation. Equivalence ratio governs mixture reactivity and heat release, affecting flame structure, reaction-zone thickness, and temperature distribution. This parameter set enables a systematic evaluation of turbulence–combustion interaction and flame stability under free-flame operation.

Table 1 Parameters used in the study.

Parameters and Symbol	Values
Diameter of swirl chamber, D	20 mm
Inlet geometry (w x h)	5 mm x 5 mm
Hydraulic diameter of double inlets, Dh	5 mm
Chamber height, H	23 mm
Equivalence ratio, ϕ	0.8, 1.0 and 1.2
Reynolds number of LPG-air mixture, Re	2,000, 4,000 and 6,000

2.3 Numerical Setup

The CFD simulations were performed using ANSYS Fluent 2023 R1 [16] to investigate the flow and combustion behavior of the premixed swirl burner. The governing equations solved included conservation of mass Equation (1), momentum Equation (2), energy Equation (3), and species transport Equation (4), together with radiation heat transfer modeled using the Discrete Ordinates (DO) approach Equation (5). Turbulence closure was provided by the RNG $k-\varepsilon$ model Equations (6)–(8), while combustion was represented using the Partially Premixed Combustion (PPC) model.

$$\frac{\partial p}{\partial t}+\nabla\cdot(pu)=0 \quad (1)$$

$$\frac{\partial}{\partial t}(\rho\vec{v})+\nabla\cdot(\rho uu)=-\nabla p+\nabla\cdot\tau+\rho g \quad (2)$$

Where τ is the viscous stress tensor.

$$\frac{\partial}{\partial t}(\rho E)+\nabla\cdot\left[(\rho E+p)u\right]=\nabla\cdot\left(k_{eff}\nabla T\right)+S_h \quad (3)$$

Where E is the total energy, k_{eff} is the effective thermal conductivity, and S_h represents energy source terms due to chemical reactions.

$$\frac{\partial}{\partial t}(\rho Y_i)+\nabla\cdot(\rho u Y_i)=-\nabla\cdot J_i+R_i \quad (4)$$

Where Y_i is the mass fraction of species i, J_i is the diffusive flux, and R_i is the net production rate due to chemical reactions.

The radiative heat transfer was modeled using the DO approach, which solves the Radiative Transfer Equation (RTE) for a finite number of discrete solid angles.

$$\frac{dI(r,s)}{ds}+(a+\sigma_s)I(r,s)=a\frac{n^2\sigma T^4}{\pi}+\frac{\sigma_s}{4\pi}\int_{4\pi}I(r,s')\Phi(s\cdot s')d\Omega' \quad (5)$$

Where $I(r,s)$ is the radiation intensity at position r in direction s, a is the absorption coefficient, σ_s is the scattering coefficient, σ is the Stefan-Boltzmann constant, and Φ is the scattering phase function.

$$\frac{\partial}{\partial t}(\rho k)+\nabla\cdot(\rho uk)=\nabla\cdot\left[\left(\mu+\frac{\mu_t}{\sigma_k}\right)\nabla k\right]+P_k-\rho\varepsilon \quad (6)$$

$$\frac{\partial}{\partial t}(\rho\varepsilon)+\nabla\cdot(\rho u\varepsilon)=\nabla\cdot\left[\left(\mu+\frac{\mu_t}{\sigma_\varepsilon}\right)\nabla\varepsilon\right]+C_{1\varepsilon}\frac{\varepsilon}{k}P_k-C_{2\varepsilon}\rho\frac{\varepsilon^2}{k}-R_\varepsilon \quad (7)$$

$$\mu_t=\rho C_\mu\frac{k^2}{\varepsilon} \quad (8)$$

Where k is turbulent kinetic energy, ε is turbulent dissipation rate, $\mu_t =$ is turbulent viscosity, P_k is production of turbulent kinetic energy, R_ε is extra correction term (RNG modification), and σ_k, σ_ε, C_μ, $C_{1\varepsilon}$, $C_{2\varepsilon}$ is empirical model constants.

For the mixing chamber (Figure 2), LPG and air were introduced through separate inlets to ensure homogeneous mixing before entering the burner. The chamber walls were defined as adiabatic with no-slip boundary conditions. The computational domain was discretized using an unstructured tetrahedral grid of ~390,000 elements (Figure 3). The corresponding boundary conditions are summarized in Table 2.

For the swirl burner (Figure 4), the premixed mixture entered through two opposing tangential inlets, generating strong swirl that enhanced mixing and stabilized the flame. The computational mesh contained ~2.5 million tetrahedral elements (Figure 5), selected after a mesh independence study. Burner walls were also set as adiabatic and no-slip. The boundary conditions are listed in Table 3.

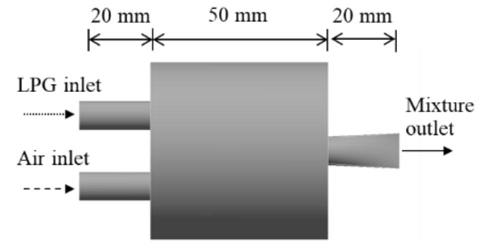

Figure 2 Geometry of the mixing chamber used in the simulation.

Table 2 Computational boundary conditions of the mixing chamber.

Boundary condition	Selected values
Inlet boundary condition	Mass flow inlet (LPG) inlet [l/min] Mass flow inlet (Air) inlet [l/min]
Outlet boundary condition	Pressure outlet (air outlet gauge, pressure outlet = 0 pa)
Solver	Pressure base
Time	Steady state
Near-wall treatment method	Standard wall function
Turbulence model	RNG $k-\varepsilon$ model
Combustion model	Species transport
Propane : butane	70 : 30
Operating condition	Operating pressure 1 atm

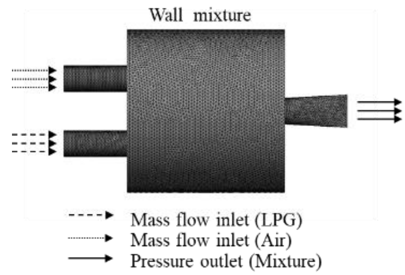

Figure 3 Boundary conditions of the mixing chamber flow model and computational mesh used in the study (390,000 elements).

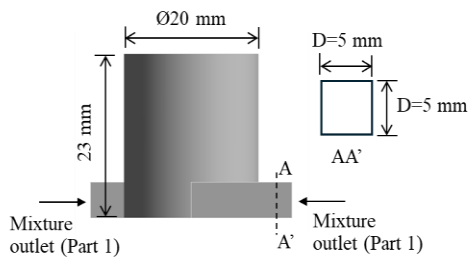

Figure 4 Geometry of the swirl burner used in the simulation.

The boundary conditions in Table 2 were selected to represent the experimental configuration and operating conditions reported by Uppatam *et al.* [5] and to maintain physical consistency with free-flame operation. Inlet boundary conditions were prescribed to match the target Reynolds numbers and equivalence ratios, using the premixed LPG-air composition and inlet temperature consistent with the experimental setup. The outlet was defined as a pressure outlet at ambient pressure to represent discharge into the surroundings without confinement. All solid surfaces were treated as

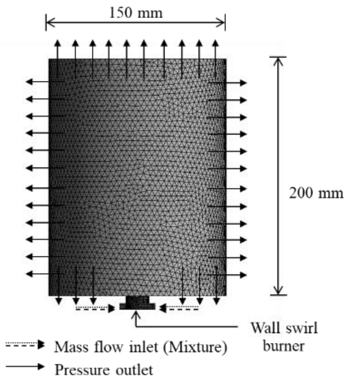

Figure 5 Boundary conditions of the swirl burner combustion model and computational mesh used in the study (2,500,000 elements).

no-slip walls to reflect the physical burner geometry. This set of boundary conditions provides a consistent numerical representation of the experimental system and supports reliable comparison between the simulated and measured results.

Table 3 Computational boundary conditions of the swirl burner.

Boundary condition	Model
Inlet boundary condition	Mass flow inlet (part 1) Mass fraction of C_3H_8, C_4H_{10}, N_2 and O_2 (Part 1)
Outlet boundary condition	Pressure outlet (air outlet gauge pressure = 0 pa)
Solver	Pressure base
Time	Steady state
Near-wall treatment method	Standard wall function
Turbulence model	RNG $k-\varepsilon$ model

Table 3 Computational boundary conditions of the swirl burner. *(continued)*

Boundary condition	Model
Combustion model	Partially premixed combustion
Radiation model	Discrete Ordinates (DO) radiation model
Operating condition	Operating pressure 1 atm

3. Results and Discussion

3.1 Model Validation

A hybrid structured-unstructured mesh of approximately 390,000 elements was generated for the premixing chamber, yielding an average wall y^+ value of 4.57, which ensured adequate near-wall resolution for turbulence modeling. For the combustion region, a mesh independence study was conducted using computational grids ranging from 0.5 to 3.0 million elements, with each case iterated for 20,000 steps. The mesh containing 2.5 million elements provided the best overall agreement with the experimental flame temperature data reported by Uppatam *et al.* [5] at axial positions Z/Dh = 2, 4, 6, 8 and 10, as illustrated in Figure 6.

The agreement between numerical predictions and experimental measurements was quantified using the Mean Absolute Error (MAE). The reported MAE of 8.19% represents the overall average across all axial positions

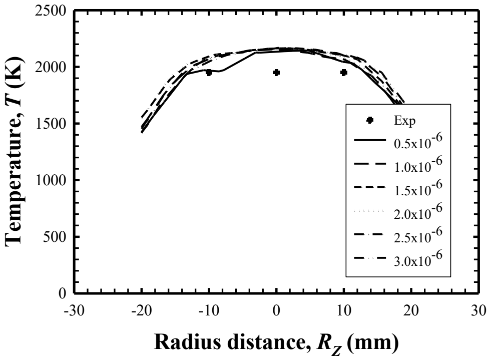

Figure 6 Comparison of simulated and experimental temperature profiles at Z / Dh = 8D.

considered, while local deviations vary with position due to differences in flame structure and temperature gradients. Despite these variations, the numerical results show good agreement with experimental data at all locations and remain within an acceptable range for turbulent premixed combustion simulations.

Increasing the grid size to 3.0 million elements did not yield further improvement in accuracy, confirming that the 2.5 million–element mesh provides an appropriate balance between accuracy and computational cost. The final mesh quality was satisfactory, with an orthogonal quality of 0.73 and a maximum aspect ratio of 13.7, ensuring numerical stability and reliable CFD predictions.

3.2 Flow and Combustion Simulation Results

Velocity contours and vector fields at the mid-plane of the mixing chamber are presented in Figure 7. Both Reynolds number and equivalence ratio (ϕ) were found to strongly influence the internal flow structures. At Re = 2,000, the flow remained quasi-laminar, with peak velocities of only 6–7 m/s and weak shear near the chamber walls, resulting in poor mixing. Increasing to Re = 4,000 led to the onset of turbulence and peak velocities of 13–15 m/s, while Re = 6,000 produced a fully developed turbulent regime with velocities above 20 m/s. The associated shear layers enhanced fuel–air mixing, thereby improving flame stability. Moreover, the increased turbulence intensity strengthens swirl-induced recirculation and promotes the transport of hot products and reactive species toward the flame root, which reinforces flame anchoring and reduces the tendency for lift-off under free-flame operation.

Figure 8 compares experimental flame images with CFD-predicted temperature fields. The results consistently reveal three distinct zones: (i) a neck zone, (ii) a reaction zone containing the peak temperature, and (iii) a post-combustion zone.

Flame structures at different equivalence ratios are illustrated in Figure 9. Lean flames ($\phi = 0.8$) were elongated and narrow, stoichiometric flames ($\phi = 1.0$) were compact and symmetric, while fuel-rich flames (ϕ =1.2), displayed thicker reaction zones with maximum temperatures approaching 2,200 K. Across Reynolds numbers,

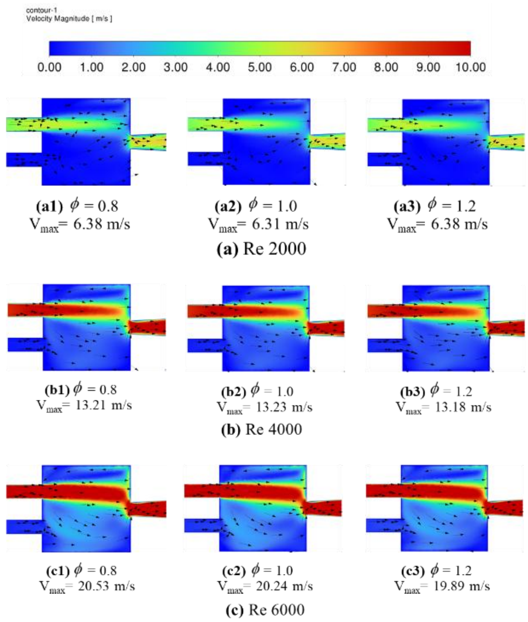

Figure 7 Velocity contours and vectors inside the mixing chamber.

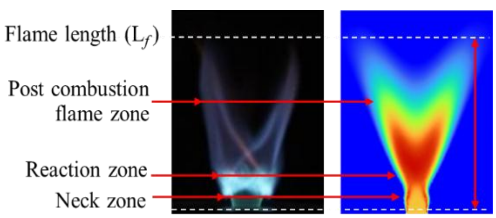

Figure 8 Comparison between experimental flame image and CFD-predicted temperature field for a free swirling flame jet.

flame stability was strongly linked to turbulence intensity: *Re* = 2,000, produced elongated, unstable flames; *Re* = 4,000, yields broader and more stable flames, and *Re* = 6,000 resulted in compact, intense flames with higher combustion efficiency. These results confirm the decisive

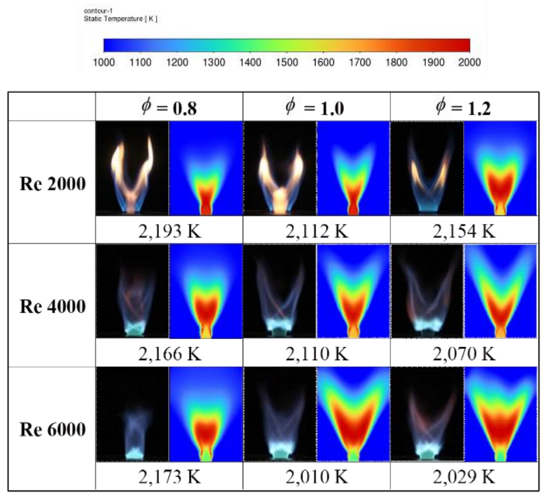

Figure 9 Comparison of experimental flame images and CFD-predicted temperature fields for different equivalence ratios.

roles of both Reynolds number and equivalence ratio in determining flame stability and structure.

3.3 Comparison of CFD Predictions with Experiments

The numerical simulations reproduced the overall flame features observed experimentally, including flame cone shape, length, and variations with equivalence ratio. Quantitatively, the temperature predictions showed MAE values within 8–10%, which is acceptable for turbulent combustion modeling. Some discrepancies were observed: in the lean case (ϕ =0.8), the CFD model predicted a lower flame liftoff height than observed experimentally, indicating slightly stronger flame anchoring in the simulations. In contrast, for the rich mixture case (ϕ =1.2), the maximum flame temperature was predicted higher than measured, suggesting overestimated heat release under fuel-rich conditions. These deviations are likely due to limitations in turbulence-chemistry interaction modeling, uncertainties in radiative heat transfer, and simplified chemistry assumptions.

Despite these localized differences, the CFD results captured the overall trends with Reynolds number and equivalence ratio, supporting the adequacy of the adopted modeling framework for LPG premixed swirl flames under free-flame operation.

It should be noted that the present simulations employ a Reynolds-averaged turbulence framework with a partially premixed combustion model, which involves inherent simplifications in turbulence–chemistry interaction and may lead to local discrepancies such as flame liftoff height and peak temperature. Future work will address these limitations by applying advanced approaches, including Large-Eddy Simulation (LES) with finite-rate chemistry or flamelet-based models, to improve prediction of local flame dynamics under free-flame conditions.

3.4 Swirl Flow

Building on the velocity and flame structure analysis presented in sections 3.2 and 3.3, the swirl number (S) was evaluated to provide a quantitative measure of the swirl intensity and its role in flame stabilization, as expressed in Equation (9). The swirl number, defined as the ratio of angular to axial momentum, governs the formation of a central recirculation zone, which is widely recognized as a key mechanism for anchoring premixed flames [2], [17].

$$S = \frac{G_\theta}{RG_x} = \frac{\int \rho U_x U_\theta r dA}{R\int \rho U_x^2 dA} \quad (9)$$

Where G_θ is the angular momentum, G_x is the axial momentum, U_x is the axial velocity, U_θ is the tangential (angular) velocity, ρ is the fluid density, r is the radius, and R is the reference radius.

Figure 11 shows the variation of swirl number with Reynolds number for different equivalence ratios. As the Reynolds number increases from 2,000 to 6,000, the swirl number increases, indicating stronger rotational motion and enhanced radial velocity near the burner exit. It is well established that a swirl number exceeding approximately 0.4 represents a critical threshold for CRZ formation, beyond which a stable central recirculation zone develops along the burner centerline. In the present study, this threshold was exceeded under high Reynolds number conditions, particularly for Re = 6,000 and ϕ = 0.8, resulting in a pronounced CRZ.

The formation of a strong CRZ significantly improves flame anchoring by continuously recirculating hot combustion products and reactive species toward the flame root. This process enhances ignition stability, shortens flame length, and increases resistance to flame lift-off and blow-off under free-flame operation. As a result, cases with swirl numbers greater than 0.4 exhibited more stable flame attachment and higher average flame temperatures compared with lower-swirl cases. These findings confirm that swirl intensity, quantified by the swirl number, is a key controlling parameter for CRZ formation and flame anchoring in LPG premixed swirl burners, directly influencing overall combustion stability and performance.

As shown in Figure 10, increasing the Reynolds number from 2,000 to 6,000 intensified radial velocity and vortex motion at the burner exit, producing stronger shear layers and more pronounced recirculation. This behavior directly contributed to enhanced flame stabilization.

Figure 11 demonstrates that, at constant Reynolds number, lean mixtures (ϕ = 0.8) consistently produced higher swirl numbers compared with stoichiometric (ϕ = 1.0) and the rich (ϕ =1.2) mixtures. This trend can be attributed to the larger airflow momentum fraction present under lean conditions. Notably, the case of Re = 6,000 and ϕ = 0.8 resulted in a

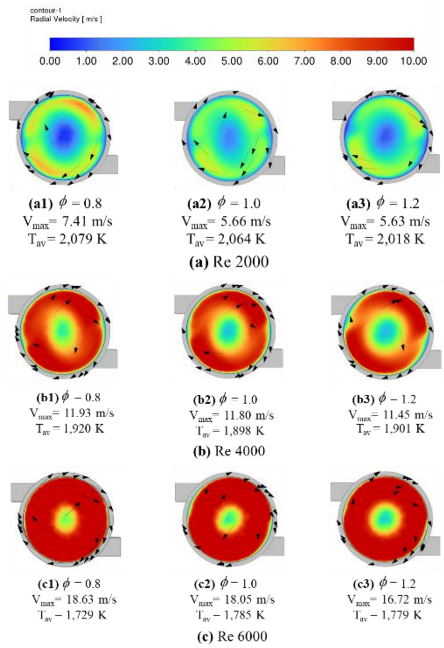

Figure 10 Radial velocity contours and velocity vectors at the burner exit.

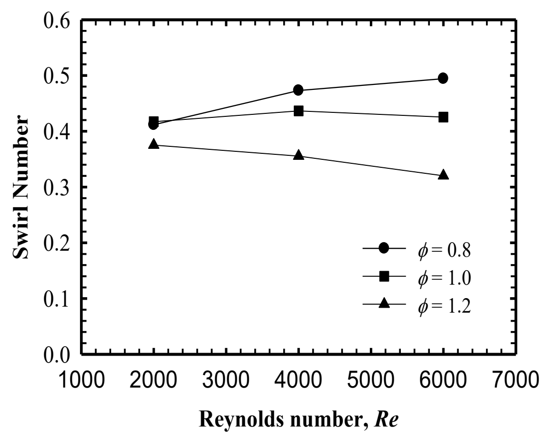

Figure 11 Variation of swirl number with Reynolds number (Re =2000,4000,6000).

swirl number exceeding 0.4, which is above the threshold required for CRZ formation. Under this condition, the flame length was shortened, mixing was enhanced, and resistance to blow-off was significantly improved.

Radial velocity distributions at the burner outlet (Figure 12) further confirmed that swirl intensity increased with Reynolds number, while temperature profiles (Figure 13) revealed that lean flames (ϕ = 0.8) achieved the highest average outlet temperatures.

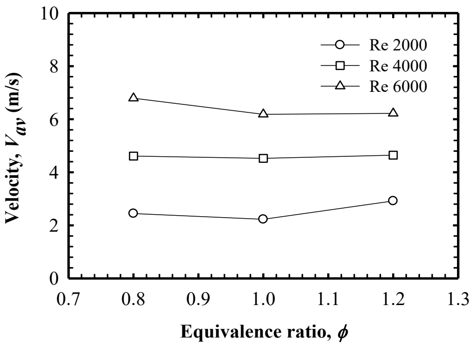

Figure 12 Variation of mean velocity with equivalence ratio at different Reynolds numbers ($Re = 2{,}000$, 4,000 and 6,000).

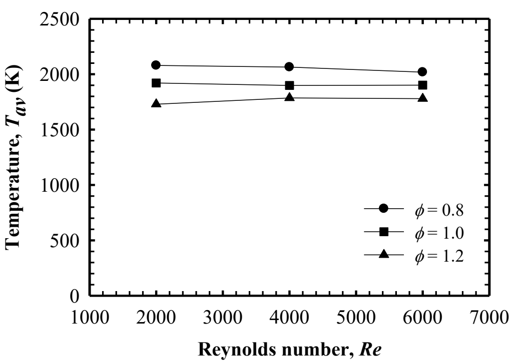

Figure 13 Variation of average flame temperature with Reynolds number at equivalence ratios ϕ = 0.8, 1.0, and 1.2.

In contrast, rich mixtures (ϕ =1.2) exhibited lower outlet temperatures due to incomplete combustion and elevated CO/UHC formation. These findings are consistent with previous studies [3], [18] and underscore the importance of swirl number optimization in improving combustion efficiency, flame anchoring, and overall burner performance.

4. Conclusion

This study numerically investigated the combustion characteristics of an LPG-fueled premixed swirl burner under free-flame conditions using a validated CFD framework. The results demonstrated that both Reynolds number and equivalence ratio play key roles in determining flame structure, stability, and thermal behavior. Increasing Reynolds number enhanced turbulence intensity and strengthened swirl-induced recirculation, leading to improved flame anchoring and stability. A central finding of this work is the critical role of swirl number in burner performance. Conditions producing swirl numbers greater than 0.4 were shown to promote the formation of a strong central recirculation zone, which significantly enhances flame anchoring by recirculating hot products and reactive species toward the flame root.In particular, lean operating conditions (ϕ =0.8) combined with sufficiently high Reynolds numbers yielded stable, compact flames with improved resistance to lift-off and blow-off, while maintaining high combustion efficiency.

From a practical burner design perspective, these findings indicate that optimizing swirl intensity to exceed the CRZ formation threshold, especially under lean mixture operation, is an effective strategy for achieving stable and efficient LPG combustion. The insights provided by this study offer useful guidance for the design and optimization of industrial LPG swirl burners, supporting the development of energy- efficient and stable combustion systems.

5. Acknowledgement

This research was financially supported by the research and innovation grant, Ubon Ratchathani University, Fiscal Year 2024

References

[1] S. Taamallah, S. J. Shanbhogue, and A. F. Ghoniem, "Turbulent flame stabilization modes in premixed swirl combustion: Physical mechanism and Karlovitz number-based criterion," *Combustion and Flame*, vol. 166, pp. 19–33, 2016, doi : 10.1016/j. combustflame.2015.12.007.

[2] B. Y. Belal, G. Li, Z. Zhang, H. M. El-Batsh, H. A. Moneib, and A. M. A. Attia, "The effect of swirl burner design configuration on combustion and emission characteristics of lean pre-vaporized premixed flames," *Energy*, vol. 228, Aug. 2021, Art. no. 120622, doi: 10.1016/j.energy.2021.120622.

[3] L. G. Becker, H. Kosaka, B. Böhm, S. Doost, R. Knappstein, M. Habermehl, R. Kneer, J. Janicka, and A. Dreizler, "Experimental investigation of flame stabilization inside the quarl of an oxyfuel swirl burner," *Fuel*, vol. 201, pp. 124–135, Aug. 2017, doi: 10.1016/j.fuel.2016.09.002.

[4] D. G. Lilley, "Swirl flows in combustion: A review," *AIAA Journal*, vol. 15, no. 8, pp. 1063–1078, Aug. 1977, doi. org/10.2514 /3.60756.

[5] N. Uppatam, W. Boonyopas, C. Aroonrujiphan, N. Kaewchoothong, S. Sae-ung, and C. Nuntadusit, "Heat transfer characteristic for premixed flame jet from swirl chamber," *Journal of Advanced Research in Fluid Mechanics and Thermal Sciences*, vol. 77, no. 2, pp. 33–46, 2020, doi: 10.379 34/arfmts.77.2.3346.

[6] M. Wichangarm, A. Matthujak, T. Sriveerakul, S. Sucharitpwatskul, and S. Phongthanapanich, "Investigation on thermal efficiency of LPG cooking burner using computational fluid dynamics," *Energy*, vol. 203, Jul. 2020, Art. no. 117849, doi: 10.1016/j.energy.2020. 117849.

[7] A. Matthujak, M. Wichangarm, T. Sriveerakul, S. Sucharitpwatskul, and S. Phongthanapanich, "Numerical investigation on the influences of swirling flow to thermal efficiency enhancement of an LPG-energy saving burner," *Case Studies in Thermal Engineering*, vol. 28, Dec. 2021, Art. no. 101466, doi: 10.1016/j.csite.2021. 101466.

[8] W. Du, S. Zhou, H. Qiu, J. Zhao, and Y. Fan, "Experiment and numerical study of the combustion behavior of hydrogen-blended natural gas in swirl burners," *Case Studies in Thermal Engineering*, vol. 39, Nov. 2022, Art. no. 102468, doi: 10.1016/j.csite.2022. 102468.

[9] A. Valera-Medina, R. Marsh, J. Runyon, D. Pugh, P. Beasley, T. Hughes, and P. Bowen, "Ammonia–methane combustion in tangential swirl burners for gas turbine power generation," *Applied Energy*, vol. 185, pp. 1362–1371, Jan. 2017, doi: 10.1016/ j.apenergy.2016.02.073.

[10] J. Cheng, C. Zong, and T. Zhu, "A comparative study of combustion models for simulating partially premixed swirling natural gas flames," *Thermal Science and Engineering Progress*, vol. 47, Jan. 2024, Art. no. 102310, doi: 10.1016/j.tsep.2023.102310.

[11] J. Zhang, C. Sui, B. Zhang, and J. Li, "Effects of swirl intensity on flame stability and NO emission in swirl-stabilized ammonia/methane combustion," *Applications in Energy and Combustion Science*, vol. 14, Jun. 2023, Art. no. 100138, doi: 10.1016/ j.jaecs.2023.100138.

[12] A. M. Steinberg, P. E. Hamlington, and X. Zhao, "Structure and dynamics of highly turbulent premixed combustion," *Progress in Energy and Combustion Science*, vol. 85, Jul. 2021, Art. no. 100900, doi: 10.1016/ j.pecs.2020.100900.

[13] D. D. Luo, H. S. Zhen, C. W. Leung, and C. S. Cheung, "Premixed flame impingement heat transfer with induced swirl," *International journal of heat and mass transfer*, vol. 53, no. 19–20, pp. 4333–4336, 2010, doi: 10.1016/j.ijheatmasstransfer.201 0.05.048.

[14] P. Kuntikana and S. V. Prabhu, "Heat transfer characteristics of premixed methane–air flame jet impinging obliquely onto a flat surface," *International Journal of Heat and Mass Transfer*, vol. 101, pp. 133–146, 2016, doi: 10.1016/j.ijheatma sstransfer.2016.05.004.

[15] A. R. Kadam, R. K. Parida, V. Hindasageri, and G. N. Kumar, "Heat transfer distribution of premixed methane-air laminar flame jets impinging on ribbed surfaces," *Applied Thermal Engineering*, vol. 163, 2019,

Art. no. 114352, doi: 10.1016/j.applthermaleng.2019.114352.

[16] Ansys Fluent. Release 2024 R2. [Online]. Available: https://www.ansys.com/blog/whats-new-ansys-fluent-software-2024-r2

[17] S. Candel, D. Durox, T. Schuller, J.-F. Bourgouin, and J. P. Moeck, "Dynamics of swirling flames," *Annual review of fluid mechanics*, vol. 46, no. 1, pp. 147–173, Jan. 2014, doi: 10.1146/annurev-fluid-010313-141300.

[18] N. Syred, "A review of oscillation mechanisms and the role of the Precessing Vortex Core (PVC) in swirl combustion systems," *Progress in Energy and Combustion Science*, vol. 32, no. 2, pp. 93–161, 2006, doi: 10.1016/j.pecs.2005.10.002.